



# Adsorption investigation of CO<sub>2</sub> on g-C<sub>3</sub>N<sub>4</sub> surface by DFT calculation



Bicheng Zhu<sup>a</sup>, Liuyang Zhang<sup>a</sup>, Difa Xu<sup>a,b</sup>, Bei Cheng<sup>a</sup>, Jiaguo Yu<sup>a,c,\*</sup>

<sup>a</sup> State Key Laboratory of Advanced Technology for Materials Synthesis and Processing, Wuhan University of Technology, Wuhan 430070, PR China

<sup>b</sup> Hunan Province Key Laboratory of Applied Environmental Photocatalysis, Changsha University, Changsha 410022, PR China

<sup>c</sup> Department of Physics, Faculty of Science, King Abdulaziz University, Jeddah 21589, Saudi Arabia

## ARTICLE INFO

### Keywords:

g-C<sub>3</sub>N<sub>4</sub>  
Density functional theory  
CO<sub>2</sub>  
Adsorption

## ABSTRACT

Photocatalytic CO<sub>2</sub> reduction is a widely studied approach applied in abating the atmospheric CO<sub>2</sub> levels and relieving energy shortage. As the first step in the process of CO<sub>2</sub> reduction, CO<sub>2</sub> adsorption plays an important role in photocatalytic activity. In the present work, the CO<sub>2</sub> adsorption ability of graphitic carbon nitride (g-C<sub>3</sub>N<sub>4</sub>) was evaluated by adsorption energy derived from first-principle calculation. To provide a more realistic result, a variety of parameters, including various adsorption sites, separation distances and rotation angles were examined to determine the most stable adsorption system. The results showed that CO<sub>2</sub> molecule preferred to adsorb at the two-coordinated nitrogen atom, which contributed to both valance band and conduction band edge. The most negative adsorption energy obtained was  $-0.4181$  eV, which is indicative of physisorption. The electronic properties of the adsorbed system were investigated, including band gap, density of states, work function, the highest occupied molecular orbital and the lowest unoccupied molecular orbital. The effects of molecular number of the adsorbate and layer number of the adsorbent on the adsorption behavior were also examined. This work provides initial and significant reference for the in-depth study of the process of photocatalytic CO<sub>2</sub> reduction on g-C<sub>3</sub>N<sub>4</sub>.

## 1. Introduction

Photocatalytic CO<sub>2</sub> reduction, which consumes CO<sub>2</sub> and produces organic fuel such as CH<sub>4</sub> and CH<sub>3</sub>OH, is a widely studied reaction [1,2]. It is contributive to relieving greenhouse effect and energy shortage [3,4]. The commonly investigated photocatalysts employed in CO<sub>2</sub> reduction include TiO<sub>2</sub> [5,6], CdS [7,8], ZnO [9,10], metal complexes [11,12] and graphitic carbon nitride (g-C<sub>3</sub>N<sub>4</sub>) [13–15]. Among these photocatalysts, g-C<sub>3</sub>N<sub>4</sub> stands out because of its unique properties such as low-cost, high stability, visible light response and layered crystal structure. However, the photocatalytic activity of pristine g-C<sub>3</sub>N<sub>4</sub> is hindered by its well-known limitations: low specific surface area and serious recombination of photogenerated electron–hole pairs.

To enlarge the surface areas of g-C<sub>3</sub>N<sub>4</sub>, many strategies have been developed, which can be summarily divided into two categories. One is designing hierarchical structures with novel morphologies [16–21]. The other is decreasing the thickness of g-C<sub>3</sub>N<sub>4</sub> nanosheets by chemical or physical exfoliation methods [22–24]. The increased surface area bestows the nanosheets with enhanced reactant adsorption. As the first step in photocatalytic CO<sub>2</sub> reduction, the adsorption of CO<sub>2</sub> on the photocatalyst is vital to photocatalytic activity [25,26]. Similar to surface area, the adsorption configuration and adsorption strength of

CO<sub>2</sub> are also imperative for the adsorption capacity and stability. However, unlike surface area, which can be determined by experimental characterizations such as nitrogen adsorption–desorption measurement, the adsorption configuration and adsorption strength of gaseous reactants on the photocatalyst are difficult to be examined by conventional experimental method. Under this scenario, first principles calculation based on density functional theory (DFT) displays irreplaceable position in the research of molecule adsorption behavior [27–29].

For photocatalytic H<sub>2</sub> production and dye degradation, Aspera et al. has already investigated the adsorption of H<sub>2</sub>O and O<sub>2</sub> on g-C<sub>3</sub>N<sub>4</sub> by DFT calculations [30,31]. Yet, for CO<sub>2</sub> adsorption, the study on g-C<sub>3</sub>N<sub>4</sub> by DFT calculations is still lacking so far, much less than the study of CO<sub>2</sub> adsorption on traditional photocatalysts (TiO<sub>2</sub> and ZnO) [32–39]. To the best of our knowledge, it is only sporadically reported in literature and only one adsorption configuration is considered [40,41]. Motivated by Aspera's pioneering work and the desire to fill this research gap, we initiated the theoretical study on the adsorption of CO<sub>2</sub> on g-C<sub>3</sub>N<sub>4</sub>. The g-C<sub>3</sub>N<sub>4</sub> surface was simulated by tri-s-triazine-based monolayer g-C<sub>3</sub>N<sub>4</sub> model due to three considerations. (1) g-C<sub>3</sub>N<sub>4</sub> has a layered crystal structure and the atomic structure in each layer is the same. (2) Tri-s-triazine-based monolayer g-C<sub>3</sub>N<sub>4</sub> model is widely used

\* Corresponding author at: State Key Laboratory of Advanced Technology for Materials Synthesis and Processing, Wuhan University of Technology, Wuhan 430070, PR China.  
E-mail address: [jiaguoyu@yahoo.com](mailto:jiaguoyu@yahoo.com) (J. Yu).

in most of the literatures on DFT investigation of g-C<sub>3</sub>N<sub>4</sub> [42–45]. (3) Monolayer g-C<sub>3</sub>N<sub>4</sub> has been experimentally synthesized and it exhibits much more excellent photocatalytic activity than bulk g-C<sub>3</sub>N<sub>4</sub> [46].

Herein, the adsorption of CO<sub>2</sub> on g-C<sub>3</sub>N<sub>4</sub> was systematically studied by first principles calculations. All kinds of possible adsorption configurations with various adsorption sites, separation distances and rotation angles were considered, and the corresponding adsorption energy was compared to determine the most stable adsorption system. The influence of the molecular number of adsorbed CO<sub>2</sub> on the adsorption behavior was also examined.

## 2. Computational method

The first principles calculations were carried out using the density functional theory. The calculations were performed within the generalized gradient approximation of Perdew–Burke–Ernzerhof (GGA-PBE) using the CASTEP module in the Materials Studio software. The ultrasoft pseudopotential was adopted to simulate the interactions between valence electrons and ionic core. A vacuum spacing of 15 Å was employed to eliminate the interactions between layers. The cutoff energy was set to be 500 eV and a Monkhorst–Pack K-point of  $3 \times 3 \times 1$  was used for geometry optimization and property calculations. During the geometry optimization, all atoms were totally relaxed without any coordinate constraints. The convergence criterions for energy, maximum force, maximum stress and maximum displacement were fixed at  $1.0 \times 10^{-5}$  eV/atom, 0.03 eV/Å, 0.05 GPa and 0.001 Å, respectively. The Heyd–Scuseria–Ernzerhof (HSE06) hybrid functional was used to obtain the accurate band structure. The adsorption energy ( $E_{\text{Ads}}$ ) of CO<sub>2</sub> adsorption on g-C<sub>3</sub>N<sub>4</sub> system is defined as [47]

$$E_{\text{Ads}} = E(\text{CO}_2\text{-C}_3\text{N}_4) - E(\text{C}_3\text{N}_4) - E(\text{CO}_2)$$

where  $E(\text{CO}_2\text{-C}_3\text{N}_4)$  and  $E(\text{C}_3\text{N}_4)$  are the total energy of g-C<sub>3</sub>N<sub>4</sub> systems with and without CO<sub>2</sub> molecule, respectively,  $E(\text{CO}_2)$  is the energy of an isolated CO<sub>2</sub> molecule. According to this definition, negative adsorption energy suggests that the adsorption process is exothermic and the adsorption system is thermodynamically stable [48]. Contrarily, a positive value corresponds to an endothermic and unstable adsorption.

## 3. Results and discussion

### 3.1. Optimized structure of g-C<sub>3</sub>N<sub>4</sub>

Pristine g-C<sub>3</sub>N<sub>4</sub> model was obtained by cleaving the unit cell of bulk g-C<sub>3</sub>N<sub>4</sub> along the (001) direction. Fig. 1 shows the geometrically optimized structure of this model which contains six carbon atoms and eight nitrogen atoms. The lattice parameter is  $a = b = 7.15$  Å, which is consistent with other calculation results [49–51]. Numbering scheme is given for convenience: three kinds of N atoms and two kinds of C atoms

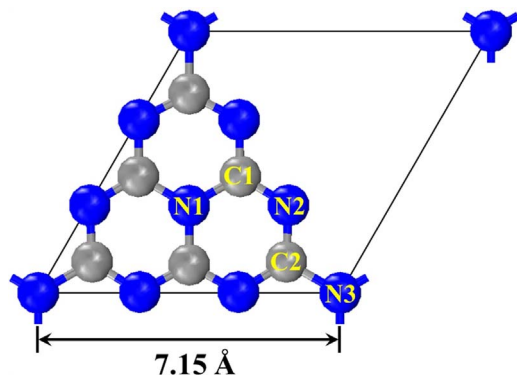


Fig. 1. Optimized structure of pristine g-C<sub>3</sub>N<sub>4</sub>. The gray and blue spheres are carbon and nitrogen atoms, respectively. (For interpretation of the references to colour in this figure legend, the reader is referred to the web version of this article.)

are labelled as N1, N2, N3, C1 and C2, respectively.

### 3.2. Construction of CO<sub>2</sub> molecule adsorbed g-C<sub>3</sub>N<sub>4</sub> model

The CO<sub>2</sub> molecule adsorbed g-C<sub>3</sub>N<sub>4</sub> models were built by placing single CO<sub>2</sub> molecule atop the g-C<sub>3</sub>N<sub>4</sub> surface. Two adsorption manners were designed, namely, the CO<sub>2</sub> molecule being parallel and vertical to the g-C<sub>3</sub>N<sub>4</sub> plane. For each adsorption manner, eleven adsorption sites were considered, including five atom sites, four bond sites, and two interstitial sites. More specifically, the five atom sites were N1, N2, N3, C1 and C2 sites; the four bond sites were the midpoints of the N1–C1, C1–N2, N2–C2 and C2–N3 bonds, which were represented as B1, B2, B3 and B4 sites; one interstitial site marked as I1 was the center of the C<sub>3</sub>N<sub>3</sub> ring, and the other interstitial site marked as I2 was the center of the six-fold cavity. Although the exact adsorption site in the actual adsorption process is multifarious and incalculable, these eleven sites are highly representative and capable to simulate all the possible adsorption situations. Moreover, these sites are commonly selected in the construction of g-C<sub>3</sub>N<sub>4</sub> based adsorption [30,31] and doping [52,53] systems.

The top views of the CO<sub>2</sub> molecule vertically adsorbed g-C<sub>3</sub>N<sub>4</sub> models are shown in Fig. 2. Since the CO<sub>2</sub> molecule is vertical to the g-C<sub>3</sub>N<sub>4</sub> plane, the C atom and one O atom in CO<sub>2</sub> molecule are covered by the other O atom in CO<sub>2</sub> molecule in the top views. The  $d$  value in Fig. 2 represents the separation distance between the g-C<sub>3</sub>N<sub>4</sub> plane and the adjacent O atom in the CO<sub>2</sub> molecule. The  $d$  values for all the vertically adsorbed g-C<sub>3</sub>N<sub>4</sub> models are 2.5 Å. The CO<sub>2</sub> molecule has a C–O bond length of 1.18 Å. The top views of the lateral CO<sub>2</sub> molecules adsorbed g-C<sub>3</sub>N<sub>4</sub> models are shown in Fig. 3. At each adsorption site, several nonequivalent and emblematic adsorption configurations were designed according to various rotation angles. In detail, there are two adsorption configurations for the N1, N3, I2 and bond sites, four for the C1, C2 and I1 sites, and six for the N2 site. The purple digits in the figures are used to mark the different configurations. The O atoms in Fig. 3 b, d, e and j are represented by spheres with relatively smaller radius to avoid the overlap of spheres. The  $d$  value in Fig. 3 indicates the separation distance between the g-C<sub>3</sub>N<sub>4</sub> plane and the CO<sub>2</sub> molecule. The  $d$  values for all the in parallel adsorbed g-C<sub>3</sub>N<sub>4</sub> models are also 2.5 Å. The N1-2 site in Fig. 3l represents the adsorption configuration marked as No. 2 at site N1 in Fig. 3a. In total, 11 vertically adsorbed models and 32 laterally adsorbed models were designed and geometrically optimized to obtain the adsorption energy for all the adsorption configurations and the adsorption energy was compared successively.

### 3.3. Adsorption energy

Table 1 shows the calculated adsorption energy for all the CO<sub>2</sub> adsorbed g-C<sub>3</sub>N<sub>4</sub> models. It is observed that all the adsorption energy is negative, indicating that the adsorption of CO<sub>2</sub> onto g-C<sub>3</sub>N<sub>4</sub> is exothermic. To sum up, the adsorption energy, except for that in N1 (−0.0453 eV) and N3 (−0.0204 eV) sites, ranging from −0.30 eV to −0.42 eV, is indicative of physisorption. These energy values are less negative than those of O<sub>2</sub> (−0.59 eV) [54] and H<sub>2</sub>O (−0.52 eV) [55] adsorption on g-C<sub>3</sub>N<sub>4</sub>, and more negative than those of H<sub>2</sub>, N<sub>2</sub>, CO and CH<sub>4</sub> adsorption (−0.078 eV to −0.163 eV) on g-C<sub>3</sub>N<sub>4</sub> [56]. It can be briefly summarized that g-C<sub>3</sub>N<sub>4</sub> exhibits relatively strong adsorption ability ( $E_{\text{Ads}}$  more negative than −0.30 eV) for CO<sub>2</sub>, H<sub>2</sub>O and O<sub>2</sub>, while weak adsorption intensity ( $E_{\text{Ads}}$  less negative than −0.163 eV) for H<sub>2</sub>, CO and CH<sub>4</sub>. Interestingly, CO<sub>2</sub>, H<sub>2</sub>O and O<sub>2</sub> are reactants in photocatalytic CO<sub>2</sub> reduction, H<sub>2</sub> production and pollutant degradation, respectively. In contrast, H<sub>2</sub>, CO and CH<sub>4</sub> are products in photocatalytic H<sub>2</sub> production and CO<sub>2</sub> reduction, respectively. Therefore, the adsorption behavior of g-C<sub>3</sub>N<sub>4</sub> corresponds to efficient adsorption of reactants and weak adsorption of products in all these photocatalytic reactions, which is very beneficial to photocatalytic performance.

Further observation shows that the adsorption energy in vertical

Download English Version:

<https://daneshyari.com/en/article/6456086>

Download Persian Version:

<https://daneshyari.com/article/6456086>

[Daneshyari.com](https://daneshyari.com)